

A BROADBAND RF CONTINUOUSLY VARIABLE TIME DELAY DEVICE

Frederick W. Freyre
Research Laboratories, Hazeltine Corporation

SUMMARY

A method for implementation of continuously variable time delay of broadband RF signals is described. The method uses Bragg Cell and optical heterodyne technology. The signal to be delayed is applied to the Bragg Cell acoustic transducer, and the delay time is the acoustic transit time from this transducer to the incident light beam. By translating the light beam, the delay is varied. Expressions describing the Bragg Cell diffraction, lens Fourier transformation, and the optical heterodyne processes are developed. Included are specifications for the variable delay including bandwidth, range of delay, and insertion loss. Applications include radar signal processing, spread spectrum intercept, radar ECM, and adaptive array antenna processing.

INTRODUCTION

Continuously variable time delay of broadband RF signals is a valuable signal processing function. Methods of achieving it include:

- o Digital - The signal is digitized, stored, and converted back to analog. This method can yield very long or infinite delays, but is bandwidth limited depending on the number of A/D and D/A converters and their speed. The length of signal delay is limited by the amount of available memory. Digital methods are characterized by large size and power consumption.
- o SAW Dispersive Transducers and Reflective Array Compressors - In one version, the signal is applied to a dispersive transducer, then frequency converted, and finally applied to another dispersive element which has equal but opposite slope. The delay depends on the LO frequency used for frequency conversion. Large insertion loss and difficulty in matching the two dispersive slopes are problem areas.
- o Magneto-Static Wave Devices - MSW devices exhibit a dispersive time delay characteristic which varies with the applied bias field. Similarly, as with the SAW approach, two dispersive elements having equal but opposite slopes are used. A delay range of 165 to 180 ns and a bandwidth of 250 MHz have been reported (Ref. 1). Difficulties lie in matching the two dispersive slopes.

A new method of achieving broadband variable delay which promises faithful signal reproduction, medium BW, and a wide range of delay uses acousto-optical and optical heterodyne technology. The delay is varied through electronic, not mechanical, means. Insertion loss is inversely proportional to the square of the laser power.

SYSTEM ARCHITECTURE DESCRIPTION

Figure 1 illustrates the system architecture. Included is a laser, a Bragg Cell, a beam translator which can include another Bragg Cell, a Fourier Transform lens, a photomixer and some mirrors and beamsplitters. The broadband signal to be delayed is applied to the Bragg Cell (B1) launch transducer. The resulting acoustic signal then propagates to a laser beam, which is incident at the cell center frequency Bragg Angle. The resulting diffracted light beams are frequency shifted by the acoustic frequencies. A beam combiner combines the diffracted beams and a local oscillator (LO) beam derived from the same laser. A Fourier Transform lens then focuses the combined beam onto a broadband semiconductor photomixer so that optical heterodyning occurs. The result is coherent signal reconstruction for those signal frequency components that are within the Bragg Cell passband and whose diffracted beams interacted with the LO. The time delay is essentially the acoustic transit time from the launch transducer to the incident light beam. Delays ranging from several nanoseconds to several microseconds are feasible. The time delay variation results from translating the incident laser beam along the length of the Bragg Cell while maintaining Bragg angle incidence. Non-mechanical electronic beam translation may be accomplished by using another Bragg Cell placed at the front focal plane of a collimating lens (Figure 2).

FOURIER TRANSFORM ANALYSIS

At Bragg Cell B1, a family of diffracted light beams is generated since $S(t)$, the signal to be delayed, is broadband. These diffracted beams are frequency shifted by the respective acoustic frequencies. The direction of frequency shift is up if the light is incident on advancing wavefronts, down otherwise. The diffraction angle θ_D for each beam is nearly proportional to the RF frequency. This angle equals $\theta_B + \Delta\theta$ (Figure 3) where

$$\sin \theta_B = \frac{\lambda}{2v_a} f_B \quad (1)$$

and

$$\Delta\theta = \frac{\lambda}{v_a} \Delta f \quad (2)$$

where θ_B = the Bragg angle for the Bragg Cell center frequency and the incident angle
 λ = the free space wavelength
 v_a = the acoustic velocity
 Δf = $f - f_B$

The acoustic signal is expressed $S(t + x_1/v_a) \exp - [j\Omega_C(t + x_1/v_a)]$ where v_a is the acoustic velocity and Ω_C the angular RF center frequency. The K vector momentum diagram appropriate to figure 3 (if we ignore beamspread angles) is shown in figure 4. An approximate expression for the amplitude of the diffracted beam outside of the A/O medium is then

$$E_d = \gamma A_d(x_1, y') S(t + \frac{x_1}{v_a}) \exp j\omega t \exp - j[\Omega_C(t + \frac{x_1}{v_a}) + \phi] \exp - j(k_d \cdot r) \quad (3)$$

where γ relates to the amplitude acousto-optic diffraction efficiency and is assumed constant over the signal bandwidth, $A_d(x'_1, y')$ is the diffracted optical beam amplitude distribution in the rotated XZ coordinate system (figure 5), ω is the optical angular frequency, and ϕ is the acoustic signal phase.

In this discussion A_d is assumed Gaussian and is expressed

$$A_d(x'_1, y') = \frac{a}{\sqrt{\pi}} \exp - a^2(y'^2 + x'^2_1) \quad (4)$$

where $a = 2/D$ and D is the optical beam diameter. From figure 5 we have

$$x'_1 = -Z \sin \theta_d + X \cos \theta_d \quad (5)$$

$$y' = y \quad (6)$$

where θ_d is the Bragg diffraction angle outside the medium. From figure 4 we have

$$\underline{k}_d \cdot \underline{r} = k(z \cos \theta_i - x_1 \sin \theta_i) + Kx_1 \quad (7)$$

where k and K are the free space optical and acoustic wavenumbers, respectively.

The spatial FT of (3) may be expressed:

$$\begin{aligned} \text{FT}(E_d) = & \gamma \exp j[(\omega - \Omega_C)t - \phi] \exp j k F \cos \theta_i \frac{a}{\sqrt{\pi}} \int \exp - a^2 y^2 \exp 2\pi v y dy \cdot \\ & \int S(t + \frac{x_1}{v_a}) \exp - a^2 (F \sin \theta_d + x_1 \cos \theta_d)^2 \exp - j \frac{\Omega_C x_1}{v_a} \cdot \\ & \exp j(k \sin \theta_i - K)x_1 \exp - j 2\pi u x_1 dx_1 \end{aligned} \quad (8)$$

where $z = -F$

F = the lens focal length

$u = x_2/\lambda F$

$v = y_2/\lambda F$

The transform along the y axis is Gaussian since

$$\text{FT}(\exp - a^2 y^2) = \frac{\sqrt{\pi}}{a} \exp - (\pi v/a)^2 \quad (9)$$

The transform along the x_2 or frequency axis is the key information. This transform equals the convolution of the transforms of each x_1 dependent factor. Recalling that $K = \Omega/v_a$ and that the transform of $\exp j a x$ is a delta function, the final result is:

$$\begin{aligned} \text{FT}(E_d) = & \gamma \exp j[(\omega - \Omega)t - \phi] \exp j k F \cos \theta_i \exp - \left(\frac{\pi v}{a}\right)^2 \cdot \\ & \text{FT} \{S(t + \frac{x_1}{v_a})\} \otimes \exp j[2\pi F \frac{\tan \theta_d}{\cos \theta_d} (u - \frac{\Omega_C}{2\pi v_a})] \cdot \exp - \left[\frac{\pi \left(u - \frac{\Omega_C}{2\pi v_a}\right)}{a \cos \theta_d}\right]^2 \end{aligned} \quad (10)$$

where \otimes is the convolution symbol.

The first part of (10) indicates that at the FT or lens back focal plan exists a frequency shifted (downshifted) light distribution. The next exponential term represents a constant phase term and is of no consequence. The v dependent term indicates (as already mentioned) that along the y_2 axis the distribution is Gaussian. The $1/e$ total width equals $4\lambda F/\pi D$. Within the bracket is the convolution of two distributions. The first which is the FT of $S(t+x_1/v_a)$ we ignore temporarily. The last term shows that along the x_2 axis a Gaussian light distribution resulting from the RF center frequency exists. Its centroid is located at the $x_2 = \lambda F \Omega_C / 2\pi v_a$. By inference, all pure sinusoids in the signal result in frequency shifted Gaussian light distributions whose centroid locations vary linearly with RF frequency. Thus, the x_2 axis is the so-called frequency axis.

A multiplicative phase term which varies non-linearly with frequency also appears immediately after the convolution sign. There will, therefore, be some distortion of the RF signal. Over a 100 MHz bandwidth for a 30 mm focal length, the phase distortion is less than 2π radians and probably not significant. Over a 10 MHz bandwidth the distortion is only about 0.1 radians.

As for $\text{FT}\{S(t+x_1/v_a)\}$, if $S(t)$ is a slowly varying function over the optical beam diameter D , the overall transform expression and the overall transform profile remain Gaussian (single frequency transform). If S is rapidly varying, e.g., pulsed RF signals whose duration is much less than the acoustic travel time through D , the shape of its transform will dominate the overall transform expression. For example, if the narrow pulse is rectangular (neglecting transducer and other bandwidth limitations) then the light distribution at the FT plane will tend toward a sinc dependence.

In this analysis it has been assumed that the lens axis bisects the incident optical beam at the Bragg Cell, as in Figure 3. This assumption is implicit in (8). But for achievement of variable delay, the incident beam is translated along the x axis and is, therefore, displaced from the lens axis. This results in an extra linear phase term in (10). The term equals $\exp - (j 2 s u)$ where s is the translated distance from lens axis, and can be shown to equal $\exp - (j \Omega t_d)$ where t_d equals the acoustic transit time between where the light intersects the acoustic beam and where the lens axis intersects the acoustic beam.

SIGNAL RECONSTRUCTION

The photomixer at the lens back focal plane is illuminated by the transformed diffracted light and a local oscillator (LO) spot. The LO light has not been frequency translated by Bragg Cell B1. The LO beam intersects the FT lens at the same location as the diffracted beams because of the action of the 2 beam splitters and 2 mirrors. Also, after reflection from the second beam splitter, the LO is approximately parallel to the diffracted beams. This guarantees that at the photomixer, the diffracted and LO light propagation directions will be nearly parallel. This parallelism is necessary for efficient optical heterodyning.

In particular, it can be shown that the photomixer current is proportional to $\text{sinc}(L \sin \alpha / \lambda)$ where α equals the misalignment angle between the 2 optical beams and L equals the spot width. As an example, if $L = 10$ microns, then α must be less than 0.9° so that the sinc function is greater than or equal to 0.9. $\lambda = 0.63$ microns was assumed. An analysis which further describes the signal reconstruction at the photomixer is given in Ref. 2.

Insertion Loss

The insertion loss expressed in decibels is the sum of the gains (losses) at the acoustic transducer, Bragg Cell, photomixer and beamsplitters. Figure 6 illustrates the system and includes some calculated and observed insertion loss data. The beamsplitter losses are included in the Bragg Cell and photomixer interactions. The acoustic transducer gain is assumed to equal -6 dB. The gain of the Bragg Cell can be expressed as

$$G_2 = \left(\frac{\pi}{\lambda}\right)^2 \frac{M_2 L P_{LASER}}{2H} \quad (11)$$

where M_2 is its A/O figure of merit, L/H is the ratio of acoustic beam width to height and P_{LASER} equals the laser power.

The gain of the photomixer can be expressed (Ref. 3) as

$$G_3 = \left(\frac{\eta e}{h\nu}\right)^2 \frac{P_{LASER} R_{eq}}{4m} \quad (12)$$

where η = the quantum efficiency

e = the electronic charge

h = Planck's constant

ν = the optical frequency

R_{eq} = the equivalent resistance of the photo detector and output circuit

$1/m$ = the fraction of the available LO power which overlaps the diffracted light

Figure 6 shows that the insertion loss varies inversely as the square of the laser power.

System Bandwidth

The bandwidth, assuming it is not limited by the Bragg Cell, is determined by the LO distribution width along the frequency axis at the photomixer. Figure 7 illustrates this characteristic. The LO spot width is essentially diffraction limited. Therefore, by narrowing the LO beam before it is focused by the FT lens, an increasingly larger spot may be obtained. This arrangement is not shown in Figure 1.

The bandwidth equals the ratio of the local oscillator spot width to the frequency gradient along the frequency axis. For a non-beamsteered Bragg Cell transducer, assuming normal Bragg diffraction, this gradient is expressed

$$\frac{\Delta x_2}{\Delta f} = \frac{F\lambda}{v_a} \Delta f \quad (13)$$

The $1/e$ Gaussian spot width equals $4\lambda F/\pi D$ where D equals the local oscillator beamwidth. Therefore, the bandwidth is expressed as

$$BW = \frac{4\lambda F/\pi D}{F\lambda/v_a} = \frac{4}{\pi} \frac{v_a}{D} \quad (14)$$

A typical bandwidth is 8 MHz. Here we assumed v_a equals 4000 m/sec and D equals 0.6 mm.

Demonstrated Results and Further Goals

Demonstrated results include:

- o 0.1 to 0.5 microsecond variable delay
- o 5 MHz bandwidth (center frequency = 80 MHz)
- o 70 dB insertion loss.

The immediate goals are:

- o reduction of insertion loss
- o increase in bandwidth
- o achievement of longer delays.

A desirable long term goal is implementation using, not discrete components, but integrated ones. The benefits of so doing are well known and relate to alignment stability, size, and long term cost.

Applications

We close this paper by listing some areas where wideband variable delay is of value. These areas include:

- o Adaptive Array Antenna Processing
- o Radar Jamming (Range Gate Pulloff)
- o Communications - Suppress Multipath Effects
- o Spread Spectrum Intercept Receiver - Feature Detection
- o Processing of Radar Signals.

REFERENCES

1. J. C. Sethares, J. M. Owens, and C. V. Smith, "MSW Nondispersive, Electronically Tunable Time Delay Elements," *Electronics Letters*, Vol. 16, No. 22, Oct. 1980, pp. 825-826.
2. J. N. Lee, N. J. Berg, M. W. Casseday, and P. S. Brody, "High-Speed Adaptive Filtering and Reconstruction of Broad-Band Signals Using Acousto-Optic Techniques," *IEEE Ultrasonics Symp. 1980*, pp. 488-491.
3. H. Melchior, M. Fisher, and F. Arams, "Photodetectors for Optical Communications Systems," *Proc. IEEE*, 58(10), Oct. 1970.

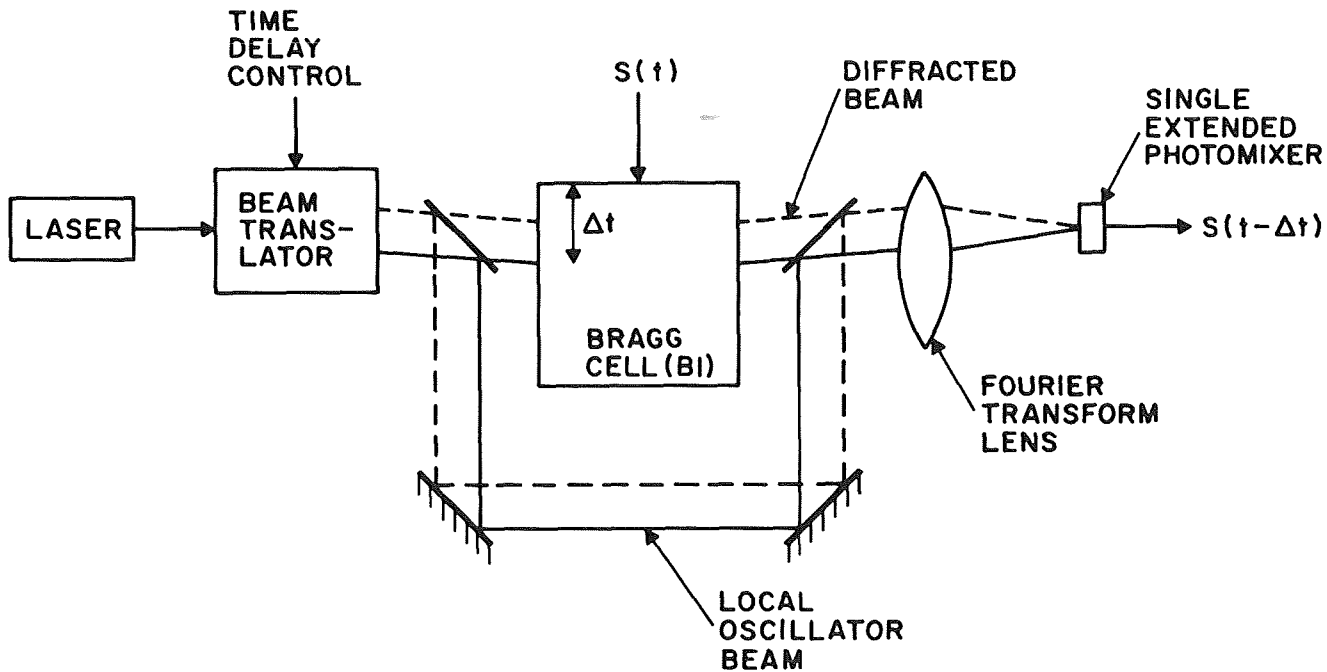


Figure 1.- A/O continuously variable wideband time delay.

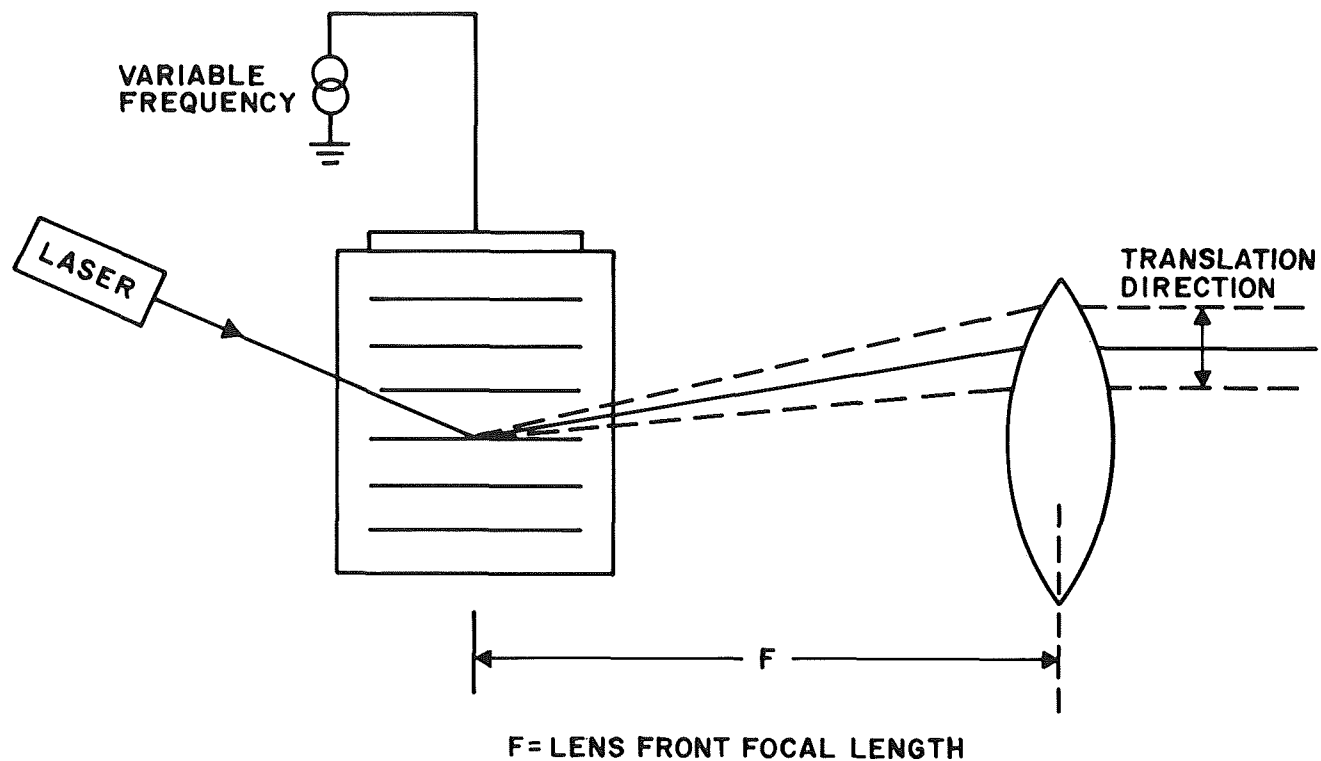


Figure 2.- Laser beam translator.

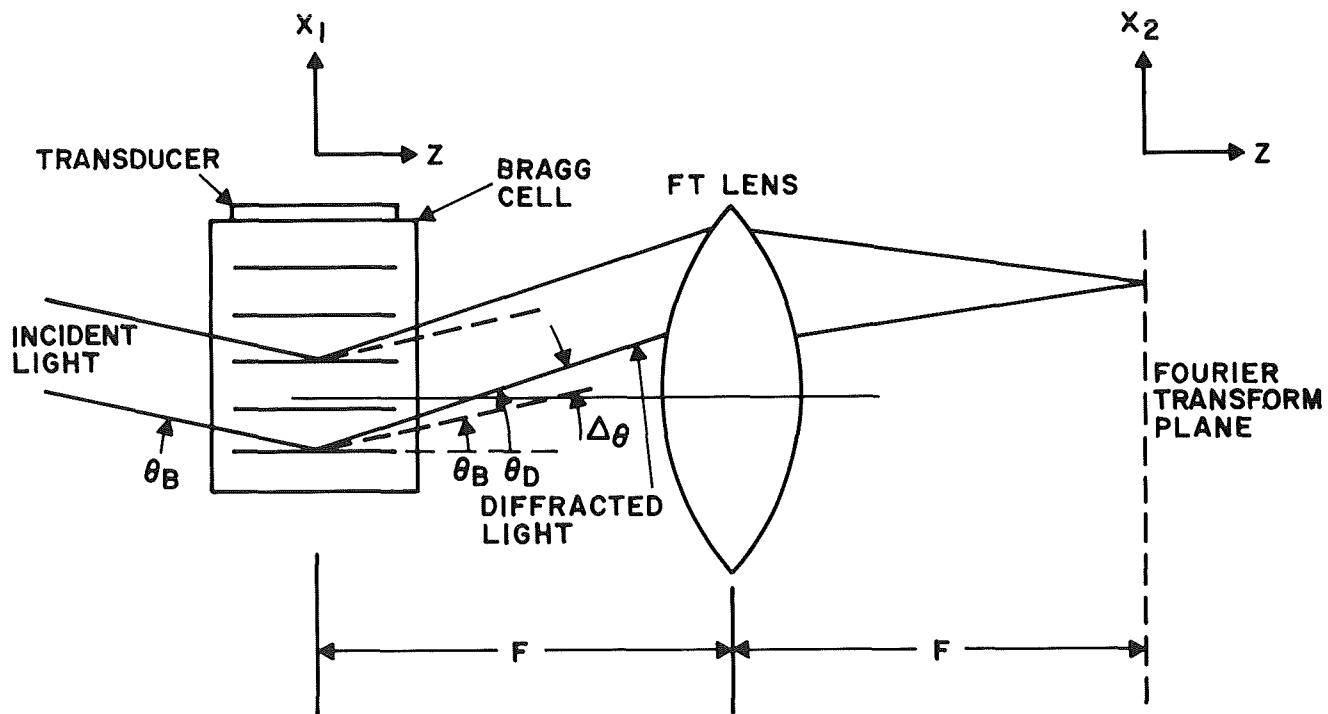


Figure 3.- Fourier transformation of Bragg diffracted light.

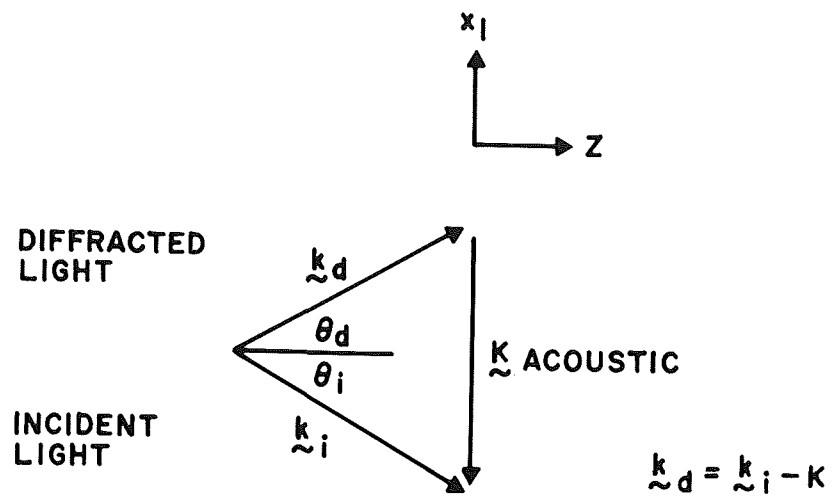


Figure 4.- Bragg diffraction momentum relation.

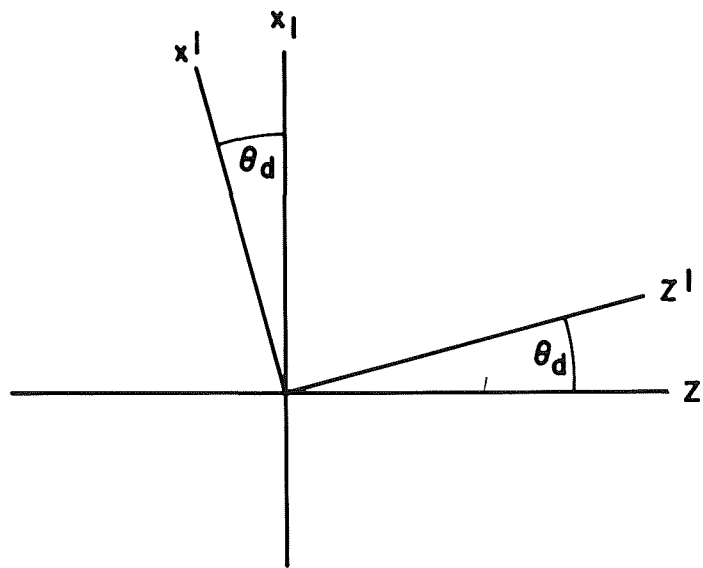
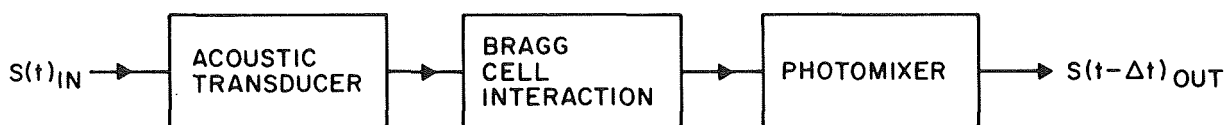


Figure 5.- Rotated XZ coordinate system.



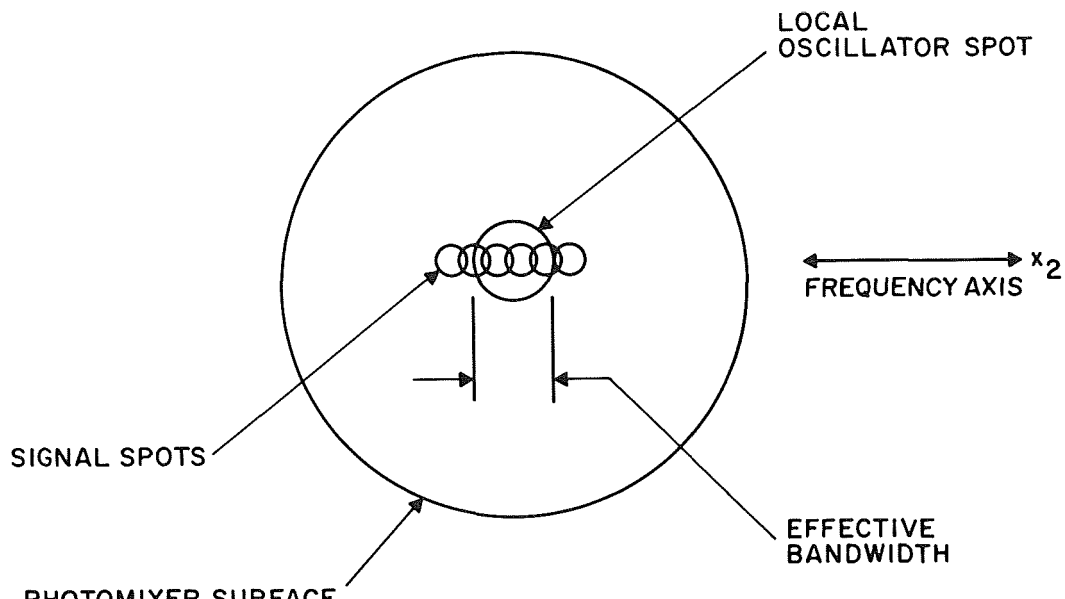
P _{LASER} (WATTS)	G ₁ (db)	G ₂ (db)	G ₃ * (db)	TOTAL THEORETICAL INSERTION LOSS	OBSERVED INSERTION LOSS
.002	-6	-25	-31	-62	-70
.020	-6	-15	-21	-42	—
.20	-6	-5	-11	-22	—

$$\text{INSERTION LOSS} = G_1 + G_2 + G_3$$

$$\text{IS PROPORTIONAL TO } \left(\frac{1}{P_{\text{LASER}}} \right)^2$$

* SIGNAL BW = 10 MHz

Figure 6.- System insertion loss.



$$\text{BANDWIDTH} = \frac{\text{LO SPOT WIDTH}}{\Delta x_2 / \Delta f}$$

Figure 7.- System bandwidth dependence.